Nanocrystalline Mesoporous Strontium Titanate as Photoelectrode Material for Photosensitized Solar Devices: Increasing Photovoltage Through Flatband Potential Engineering

ARTICLE *in* THE JOURNAL OF PHYSICAL CHEMISTRY B · OCTOBER 1999

Impact Factor: 3.3 · DOI: 10.1021/jp9913867 · Source: OAI

Nanocrystalline Mesoporous Strontium Titanate as Photoelectrode Material for Photosensitized Solar Devices: Increasing Photovoltage through Flatband Potential Engineering

Shelly Burnside,* Jacques-E. Moser, Keith Brooks, and Michael Grätzel

Laboratory for Photonics and Interfaces, Ecole Polytechnique Federale de Lausanne, 1015 Lausanne, Switzerland

David Cahen

Department of Materials and Interfaces, Weizmann Institute of Science, Rehovot 76100, Israel

Received: April 28, 1999; In Final Form: July 1, 1999

Nanocrystalline $SrTiO_3$ is synthesized by hydrothermal treatment of nanocrystalline titanium dioxide in the presence of strontium hydroxide. Working photoelectrochemical solar cells are produced using these nanometer-sized semiconductor particles as photoelectrode materials. At AM 1.5, measured open circuit voltages were roughly 100 mV higher than in solar cells produced using nanocrystalline titanium dioxide (anatase), in agreement with a simple relation between semiconductor conduction band edge and open circuit voltage for these cells. Photocurrents measured in the $SrTiO_3$ cells were roughly 1/3 those measured with TiO_2 (anatase) -based cells. On the basis of flash laser photolysis and absorptance studies, we suggest that low dye loading and possibly suboptimal dye−oxide interactions can be the cause for the relatively low photocurrents in the $SrTiO_3$ system.

Introduction

Dye-sensitized solar cells (DSSCs) present a promising alternative to current solar technologies.[1] The fundamental component of the DSSC is a photoelectrode consisting of a monolayer of a photosensitizer (S) (typically a ruthenium bipyridyl complex) adsorbed onto a 5−15 micron thick porous layer of nanocrystalline mesoporous semiconductor (SC) oxide particles. For these devices, the absorbed photon-to-electron conversion efficiency (APCE) is controlled by a series of competitive electron transfer processes. Following light absorption by adsorbed dye molecules (eq 1), electron injection from the excited state of the sensitizer to the conduction band of the semiconductor (eq 2) competes kinetically with the deactivation of the excited state (eq 3). Dye regeneration and concomitant oxidation of the iodide-containing redox mediator (eq 4) further compete with the interfacial charge recombination reaction that takes place between conduction band electrons and dye cations (eq 5). Finally, charge transport by the electrolyte in the pores of the nanocrystalline semiconductor film and that of the injected electrons within the solid, to the back contact of the semiconductor and to the counterelectrode, respectively, should be fast enough to compete efficiently with the recombination reaction (eq 6).

$$S|SC + h\nu \rightarrow S^*|SC \quad (1)$$

$$S^*|SC \rightarrow S^+|SC + e^-_{cb}\,(SC) \quad (2)$$

$$S^*|SC \rightarrow S \quad (3)$$

$$S^+|SC + 3/2\ I^- \rightarrow S + 1/2\ I_3- \quad (4)$$

$$S^+|SC + e^-_{cb}\,(SC) \rightarrow S|SC \quad (5)$$

$$e^-_{cb}\,(SC) + 1/2\ I_3- \rightarrow 3/2\ I^- \quad (6)$$

The anatase phase of TiO_2, with a band gap of 3.2 eV, is often used as a photoelectrode semiconductor material and has yielded DSSCs with efficiencies of over 10%.[2,3] The difference in energy between the Fermi level of the photoelectrode semiconductor oxide and the redox potential of the electrolyte equals the theoretical maximum open circuit voltage (V_{oc}) which can be obtained from devices containing semiconductor−electrolyte interfaces, such as DSSCs (Figure 1a).[4] If we take the flatband potentials as an approximation to the (quasi) Fermi level of an illuminated semiconductor, a DSSC flatband potential should correlate with the cell's V_{oc}.[4] In an investigation of a variety of oxides,[5] such a correlation was found for ZnO, Nb_2O_5, and SnO_2, with typically poorer efficiencies than for TiO_2.[6−8]

In comparison with these binary oxide semiconductors, the ternary oxide strontium titanate ($SrTiO_3$) shares more structural similarities with anatase and can be loosely thought of as a highly doped TiO_2 structure. This perovskite material contains titanium atoms in 6-fold octahedral coordination, similar to the titanium arrangement in anatase. The two materials have identical band gaps, but strontium titanate has a slightly higher flatband potential and thus we expect a higher V_{oc} for a $SrTiO_3$-based DSSC than for an anatase-based one (Figure 1b). With its higher flatband potential, $SrTiO_3$ is capable of photoassisted electrolysis of water, in contrast with anatase.[4] Also, sensitized polycrystalline $SrTiO_3$ electrodes on titanium rods have been studied previously in aqueous electrolytes and shown to yield higher V_{oc} than porous anatase films on Ti foils.[9] However, photocurrents in this $SrTiO_3$ material (with unknown crystallite size and porosity) were discouragingly low.

In this work, we demonstrate the preparation of mesoporous films of nanometer-sized particulate $SrTiO_3$. The photovoltaic behavior of DSSCs prepared with these films is then compared to that of similar anatase TiO_2-based cells. The purpose of such comparison is two-fold. First, we wish to check, in as controlled

10.1021/jp9913867 CCC: $18.00
Published on Web 08/13/1999

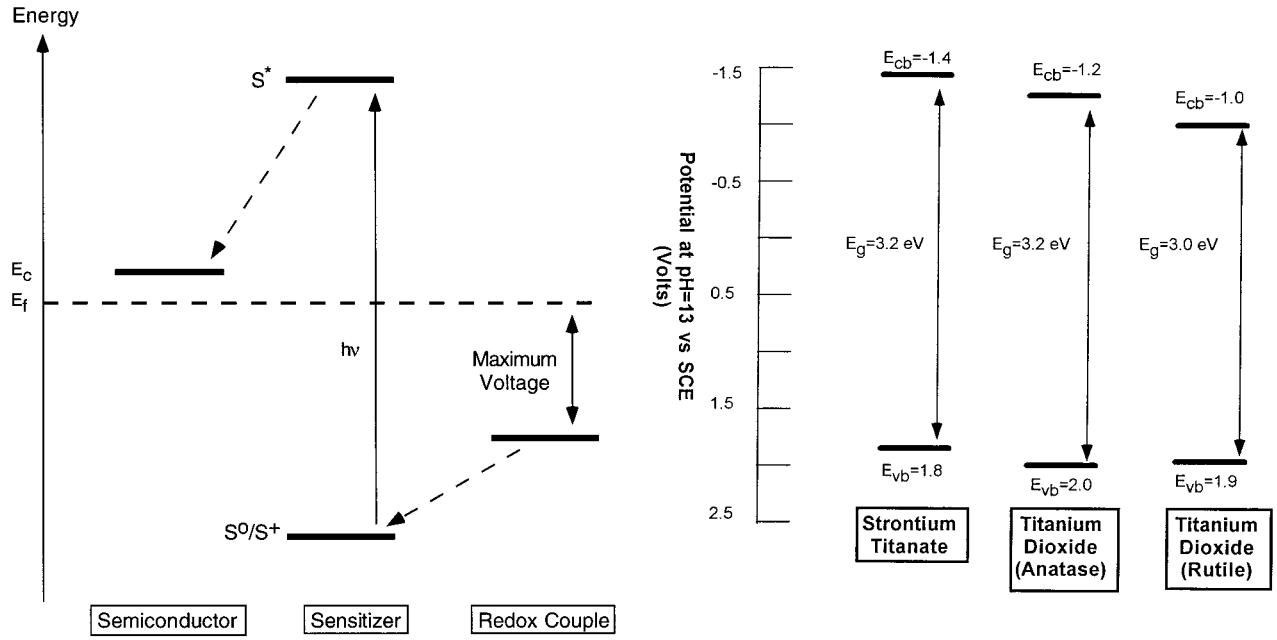

Figure 1. (a) Energy level scheme of a DSSC. E_c is the bottom of the conduction band of the semiconductor and E_f is the Fermi level of the semiconductor. (b) Energy level comparison of strontium titanate, anatase, and rutile. Data from refs 13 and 14.

a manner as possible, the simple energetic picture of the DSSC V_{oc}, mentioned above. Second, we reexamine the viability of $SrTiO_3$-based DSSCs in light of recent advances in the optimization of photoelectrode mesostructure, sensitizer, and electrolyte materials.

Experimental

Strontium titanate was prepared using a slightly modified previously published technique.[10,11] Strontium hydroxide (2.04 g) (97%, Alfa) was dissolved in 50 mL boiling distilled water which had been degassed previously with nitrogen gas for at least 30 min. A colloidal suspension containing 0.0169 mol of suspended titanium dioxide (surface area 188 m^2/g) in distilled water which had been adjusted to pH = 13 using tetramethylammonium hydroxide (Fluka) was synthesized using a previously described technique.[12] The strontium hydroxide solution was then added to 5 mL of the titanium dioxide suspension, which had also been degassed with nitrogen gas for at least 30 min before mixing the two liquids. Upon addition of the strontium hydroxide solution, the previously translucent titanium dioxide suspension turned milky white. This suspension was stirred at room temperature for at least 12 h before autoclaving in a Teflon lined titanium autoclave at 190 °C for 4.5 h. The resultant liquid was an unstable suspension of milky white colloid. Fifteen mL (15.51 g) of this suspension was combined with 1.42 g of a 10% solution of hydroxypropyl cellulose (avg M_w = 100 000, Aldrich) in water. The liquid was slowly evaporated using a rotoevaporator, until the resultant suspension contained 50% colloid by weight. Translucent films were deposited on plain glass or conducting glass (SnO_2:F-coated TEC 15 from Libbey-Owens-Ford) using a doctor blading technique. The films were sintered on a titanium hot plate (Bioblock Scientific) at temperatures between 500 and 600 °C in a flowing oxygen atmosphere. Pure titanium dioxide (anatase) films were also synthesized and deposited using previously described techniques.[2]

X-ray analysis was performed with a Siemens powder X-ray diffractometer using Cu Kα radiation. N_2 adsorption/desorption analysis was performed using a Micromeritics ASAP 2010. SEM micrographs were obtained on films deposited on conducting glass using a Hitachi S-900 field emission microscope. High-resolution transmission electron microscopy was performed using a Philips CM 30 ST.

Films deposited on conducting glass were soaked for at least 4 h in an ethanolic solution of ruthenium sensitizer (ruthenium (2,2′-bipyridyl-4,4′-dicarboxylate)$_2$(NCS)$_2$). After being removed from the dye solution, the electrode was rinsed and dried. As will be shown and explained below, dye uptake of the $SrTiO_3$ films was about half of that of the anatase films. A drop of an electrolyte solution was placed on the electrode, which quickly penetrated the film. The electrolyte solution contained 0.6 M dimethylpropylimidazolium iodide, 100 mM LiI (Fluka), 100 mM I_2 (Fluka), and 0.5 M *tert*-butylpyridine (Fluka) in methoxyacetonitrile (Fluka). A platinized counterelectrode was clipped on the working electrode before measuring the current−voltage characteristics and action spectra of these cells at AM 1.5 (∼1 Sun). The equipment used to measure the current−voltage response of the photovoltaic cells has been described previously.[3] For flash photolysis studies, the surface of the photosensitized strontium titanate samples was covered by a film of dry glutaronitrile (Fluka, distilled once) or dry glutaronitrile containing 0.5 M tetrabutylammonium iodide (Fluka), and protected by a thin microscope coverglass. Although rather turbid and poorly colored, the obtained samples were found to be usable in conventional transient absorbance experiments. Pulsed laser excitation was applied using a GWU-350 broadband optical parametric oscillator pumped by a Continuum Powerlite 7030 frequency-tripled Q-switched Nd:YAG laser (λ = 355 nm, repetition rate 30 Hz). The output of the OPO (pulse width at half-height ∼ 5 ns) was tuned at λ = 600 nm and attenuated to 0.5 mJ/pulse. The beam was expanded by a planoconcave lens to irradiate a large cross-section (approximately 1 cm^2) of the sample, whose surface was kept at a 45° angle to the excitation and to the analyzer light. The probe beam, produced by a cw 450 W Xe-arc lamp, was passed through various optical elements, the sample, and a monochromator, prior to being detected by a fast photomultiplier tube. A 1 GHz band-pass digital oscilloscope was employed to record the time course of

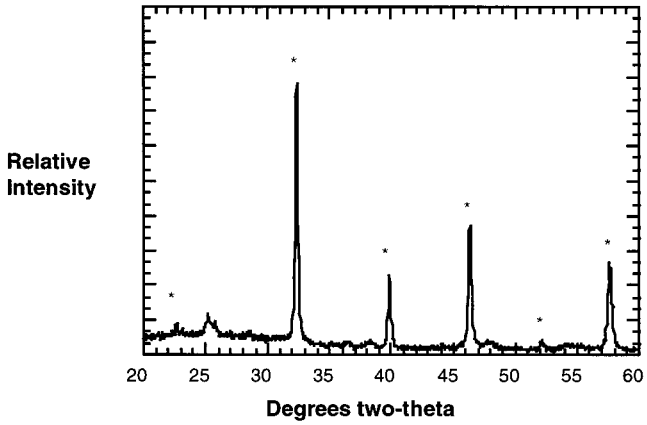

Figure 2. X-ray analysis pattern of colloids. Strontium titanate peaks are marked with an asterisk (*), the remainder of the peaks can be indexed to strontium carbonate and titanium dioxide (anatase phase).

the optical absorbance changes induced by pulsed laser excitation of the films. Satisfactory S/N ratios were typically obtained by averaging over 10−200 laser shots. Diffuse reflection and transmittance spectra of photosensitized strontium titanium were recorded on a Varian Cary 5 UV−Vis−NIR spectrophotometer equipped with a Spectralon-coated integrating sphere.

Results and Discussion

X-ray diffraction analysis (Figure 2) shows that the synthesized colloids contain $SrTiO_3$ with the perovskite structure (synthetic tausonite, JCPDS card 25-734) with traces of $SrCO_3$ (synthetic strontianite, JCPDS card 5-418) and TiO_2 (anatase, JCPDS card 21-1272). Their surface area, as modeled with the BET equation, was determined to be 85 m^2/g. A particle diameter of 14 nm can be calculated from the surface area, assuming uniform spherical particles and using a density of 5.11 g/cm^3 for $SrTiO_3$ (JCPDS card 25-734). Film porosity was calculated to be 60%. SEM images (Figure 3a) of the translucent films reveal a bimodal particle distribution, with small, roughly spherical particles, between 10 and 15 nm in diameter, and larger cubic particles, reflecting the cubic crystal phase, which measure 40−60 nm along a side. The bimodal distribution is highly desired in DSSCs for optimal balance between high dye adsorption and increased light scattering that increases the optical path length in the photoelectrode.[2] High-resolution transmission electron microscopy (HRTEM) of these particles showed them to be monocrystals. By a simple doctor-blading technique, 5−6 μm thick films of these strontium titanate films could be deposited.

Titanium dioxide films were used as a comparison (Figure 3b). Phase-pure anatase colloids were synthesized using procedures described earlier.[2,12] The individual particles are monocrystals, as shown using HRTEM. Using a screen printing technique, films were deposited which were 7−10 μm in thickness. Nitrogen adsorption/desorption measurements of these films revealed a particle surface area of 75 m^2/g and a film porosity of 60%.

Representative results of photovoltaic measurements of sensitized strontium titanate films in DSSCs at AM 1.5 are shown in Table 1 and Figure 4. Results from a mesoporous nanocrystalline anatase film-based DSSC measured under the same conditions are shown for comparison. The open circuit voltage is roughly 100 mV higher with the strontium titanate than with the titanium dioxide DSSC. All $SrTiO_3$-based DSSCs yielded V_{oc} values of between 785 and 810 mV at AM 1.5. The fill factor for the strontium titanate cells is also higher than for anatase cells, indicating lower internal resistances and higher diode ideality factors in the $SrTiO_3$ cells. In contrast, the short-circuit current and incident photon-to-electron conversion efficiency (IPCE) values for the strontium titanate-based cells are less than one-third of those obtained with titanium dioxide, resulting in a lower overall efficiency. As the preceding characterization of these two samples shows no large differences in particle size, surface area, or film thickness, the differences in photovoltaic behavior must arise from intrinsic differences between dye-coated TiO_2 and $SrTiO_3$.

We ascribe the increased open circuit voltage measured to the higher flatband potential of $SrTiO_3$ ($V_{fb} = -1.4$ V vs SCE at pH 13 [13]) as compared to that of TiO_2 (anatase) ($V_{fb} = -1.2$ V vs SCE at pH 13 [14]). This idea agrees with the theoretical picture described in Figure 1a. Literature values for flatband potentials have a wide scatter, but we have taken two values obtained for single-crystal materials via Mott−Schottky plots of interfacial capacitance vs potential, a measurement technique considered to be one of the most reliable determinations of flatband potentials. Polycrystalline anatase films, measured using an optical technique in aqueous solvents, have also been shown to have flatband potentials similar to single-crystal materials.[15] The flatband potentials compared herein have been for aqueous solvents, as these values are the most unambiguous and trusted. However, the same trend ($SrTiO_3$ > anatase > rutile) can be observed in the literature reports of flatband potentials in acetonitrile and other aprotic solvents, suggesting a more universal trend which would hold true also in the mixed solvent system used herein.[4,14,16] While our conclusions agree with those drawn in ref 5, we note that when making comparisons with titanium dioxide samples (cf. ref 5), it is important to utilize the flatband potential of the correct crystal phase, as many unspecified literature values actually refer to rutile.

Even though the currents and IPCE values obtained here with $SrTiO_3$ far exceed those reported hitherto, they are poor compared to those obtained in today's optimized anatase-based cells. As, a priori, the difference in energetics between $SrTiO_3$ and anatase should not affect the electron-transfer dynamics in the cells, we examined this matter further. Laser flash photolysis was used on dye-sensitized porous $SrTiO_3$ films deposited on glass substrates to monitor the dynamics of eqs 2−5 individually, and thus to provide a quantitative estimate of the quantum yield for electron injection in the semiconductor[17,18] and for transfer of an oxidative equivalent to the electrolyte mediator. Traces A and C in Figure 5 show transient absorbance signals recorded at $\lambda = 500$ nm upon pulsed laser irradiation of a dye-sensitized $SrTiO_3$ sample in glutaronitrile with no electrolyte added. Bleaching of the sensitizer's ground state occurs within the laser pulse duration on a nanosecond time scale. No faster kinetic component could be distinguished. For comparison, Trace B shows the transient signal obtained upon excitation of the same dye adsorbed on ZrO_2 in similar conditions. Charge injection in zirconia is not thermodynamically feasible, and, as a result, the ground-state absorption of the dye is promptly recovered by deactivation of the excited state (eq 3), whose lifetime on the oxide surface is estimated to be $\tau_{1/2} \cong 15$ ns.[18,19] From the very long lifetime of the bleaching signal observed for the dye adsorbed on $SrTiO_3$, it is thus concluded that charge injection (eq 2) does indeed occur quantitatively ($\Phi_{inj} > 0.8$) into this material. The slow recovery of the initial absorbance of the adsorbed dye is attributed to the back electron transfer reaction (eq 5). The half-lifetime of this process on nanocrystalline strontium titanate, $t_{50\%} \cong 150$ μs, is comparable to what has been reported for the same sensitizer adsorbed on TiO_2.[19]

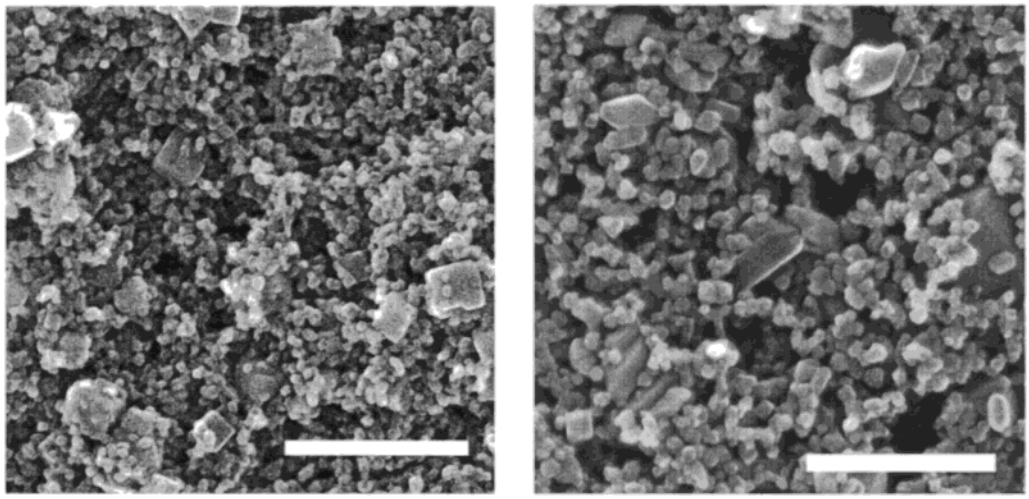

Figure 3. (a) SEM image of nanocrystalline strontium titanate; (b) SEM image of nanocrystalline titanium dioxide (anatase). Scale bar = 200 nm for both images.

TABLE 1: Results of Photovoltaic Measurements on DSSCs Based on Strontium Titanate and on Anatase Titanium Dioxide, at AM 1.5 (~1 Sun)

semiconductor oxide	V_{oc} (mV)	I_{sc} (mA/cm^2)	fill factor	efficiency (%)	IPCE @ 540 nm (%)
strontium titanate	789	3	0.70	1.8	23.1
titanium dioxide (anatase)	686	13	0.63	6.0	72.8

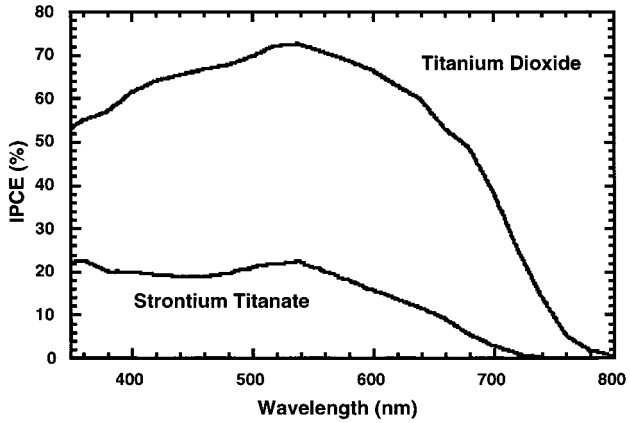

Figure 4. IPCE (incident photon-to-current efficiency) of sensitized $SrTiO_3$ and TiO_2 films. IPCE values were calculated using IPCE = (1250 × photocurrent density [μA/cm^2])/(wavelength [nm] × total, incident photon flux [W/m^2]).

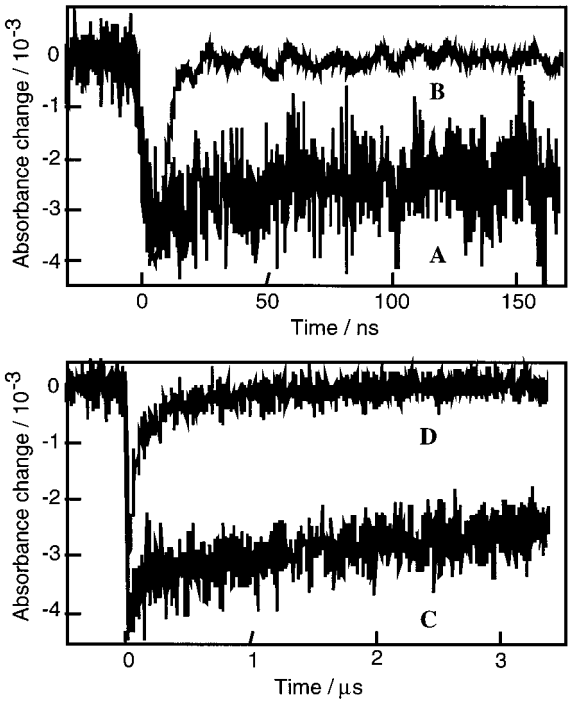

Figure 5. Transient absorbance changes observed at $\lambda = 500$ nm upon ns laser excitation of a dye-sensitized nanocrystalline layer of $SrTiO_3$ in glutaronitrile, with no electrolyte added (Traces A and C), and in the presence of 0.5 M tetrabutylammonium iodide (Trace D). For comparison, Trace B shows the signal obtained upon pulsed laser excitation of the same sensitizer adsorbed on ZrO_2 nanocrystalline film in similar conditions (glutaronitrile, no electrolyte), where no charge injection occurs.

On nanocrystalline strontium titanate films, addition in the solvent of 0.5 M tetrabutylammonium iodide as an electrolyte causes a drastic reduction of this lifetime to $t_{50\%} \cong 30$ ns (Trace D). This fast recovery of the dye ground-state absorption indicates that the iodide mediator is able to quickly intercept the sensitizer's oxidized state (eq 4), thus competing efficiently with the charge recombination process (eq 6), whose rate constant is slower by 3 orders of magnitude. As both charge injection and dye regeneration processes do take place with quantum yields approaching unity, these two steps are therefore not likely to control the overall photon-to-current conversion efficiency.

In view of these findings, it appears that the relatively low photocurrents most likely arise from low dye uptake on the $SrTiO_3$ in comparison with that on the TiO_2, as the other physical parameters, including particle size, surface area, and film thickness, are roughly similar and cannot account for the large differences in photocurrent. To check this hypothesis, absorptance values were calculated following the measurement of transmission and reflection spectra of sensitized $SrTiO_3$ films using a spectrometer equipped with an integrating sphere (absorptance (λ) = 1 − reflectance (λ) − transmitance (λ)) (Figure 6). The maximum of the absorptance spectrum was found to be low (roughly 40%), in comparison with absorptance values of over 80% for TiO_2.[20] As the maxima of the IPCE and absorptance spectra are at roughly the same wavelength, division of the IPCE spectrum (maximum 25%) by absorptance (maximum 37%) yields an acceptable APCE spectrum, with maximal values of roughly 70%. On the basis of these results, we suggest that higher absorptance values, and thus higher IPCE values,

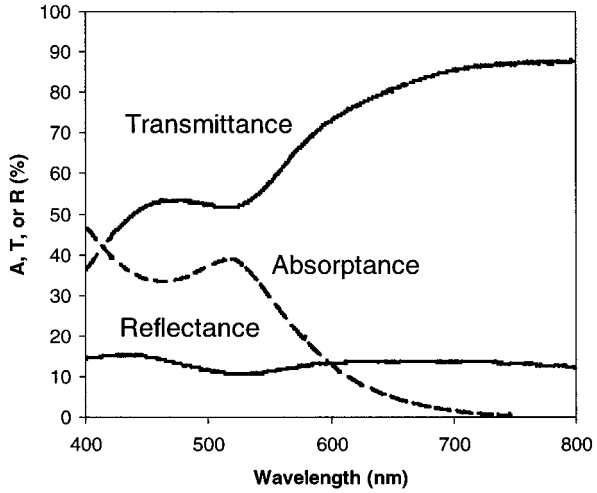

Figure 6. Experimental reflectance (R) and transmittance (T) spectra of sensitized strontium titanate films on conducting glass and the absorptance (A) spectrum calculated from these.

can be achieved with thicker films with the addition of larger or more scattering particles to increase the path length of photons in the film,[2] and/or by increasing dye uptake on the $SrTiO_3$ film. It is possible that the low dye uptake is connected with an interfacial problem between the dye and the oxide surface. The (001) surface of $SrTiO_3$, favored energetically over the more polar (111) surface,[21,22] has two possible terminations, SrO or TiO_2, both observed experimentally and neither strongly energetically favored.[21,23] As the more basic SrO surfaces poorly adsorb the negatively charged carboxylate group of the sensitizer, their presence will lead to decreased dye uptake by the semiconductor. We suggest that both strontium- and titantium-rich surfaces exist in our sample, as we have taken no precautions to tailor the surface. Additionally, we note that the Ti−Ti distances in $SrTiO_3$ (0.3905 nm) are slightly larger than in anatase (0.378 nm), which may lead to difficulties in dye adsorption through the bridging carboxylate structure often assumed for sensitizer adsorption.[24,25] A shift away from the bridging structure to a monodentate adsorption may lead to steric complications not observed in anatase. As a final remark on dye uptake, we note that the lower dye uptake of the $SrTiO_3$ films as compared to the anatase cells will influence the photovoltage much less than the photocurrent, as the photovoltage is logarithmically dependent upon the light-induced current via the Ideal Diode equation. Therefore, as the light-induced current can be related directly to the dye coverage of the films, the lower dye coverge of the $SrTiO_3$ will actually *lower* the photovoltage. This implies that the experimentally observed higher photovoltage of the $SrTiO_3$ films, as compared to the anatase films, is only a lower limit to the band edge effect schematically depicted in Figure 1a.

Conclusion

Translucent, well-characterized, nanocrystalline mesoporous films of strontium titanate have been deposited on conducting glass substrates from colloidal suspensions and assembled into DSSCs, which show encouraging V_{oc} values. These results are interpreted in terms of the higher flatband potential of $SrTiO_3$ in comparison with anatase. Differences between the photovoltaic behavior of the two semiconductors have been explained in terms of intrinsic differences between the two sensitized materials, as precautions have been taken to ensure the samples are roughly similar in physical (film and colloidal) characteristics.

Flash laser photolysis and absorptance studies imply the low photocurrents observed result from poor dye uptake by the $SrTiO_3$ surface but not from fundamental electron injection or transport problems in the semiconductor. Recent work has suggested that the $SrTiO_3$ surface can be selectively altered through pH treatments to etch the more acidic TiO_2 or the more basic SrO, and future syntheses which minimize the SrO-terminated surfaces may enhance dye adsorptance values and increase photocurrents and IPCE values.[26] Alternately, the sensitizer used has been optimized for anatase, and use of other sensitizers may lead to improved performance through better interfacial characteristics.

Acknowledgment. We thank Dr. Valery Shklover for the SEM and TEM studies, Dr. Marie Jirousek for measuring the photovoltaic performance, and Pascal Comte and Francine Arendse-Duriaux for providing the TiO_2 sample. Funding has been supplied by the Swiss National Office of Energy (OFEN). D.C. thanks the EPFL for a visiting professorship.

References and Notes

(1) O'Regan, B.; Grätzel, M. *Nature* **1991**, *353*, 737−739.
(2) Barbe, C. J.; Arendse, F.; Comte, P.; Jirousek, M.; Lenzmann, F.; Shklover, V.; Grätzel, M. *J. Amer. Cer. Soc.* **1997**, *80*, 3157−3171.
(3) Nazeeruddin, M. K.; Kay, A.; Rodicio, I.; Humphry-Baker, R.; Mueller, E.; Liska, P.; Vlachopoulos, V.; Grätzel, M. *J. Am. Chem. Soc.* **1993**, *115*, 6382−6390.
(4) Finklea, H. O. *Semiconductor Electrodes*; Elsevier: Amsterdam, 1988; Vol. 55.
(5) Sayama, K.; Sugihara, H.; Arakawa, H. *Chem. Mater.* **1998**, *10*, 3825−3832.
(6) Bedja, I.; Hotchandani, S.; Kamat, P. V. *J. Phys. Chem.* **1994**, *98*, 4133−4140.
(7) O'Regan, B.; Schwartz, D. T. *J. Appl. Phys.* **1996**, *80*, 4749−4754.
(8) Rensmo, H.; Keis, K.; Lindstrom, H.; Sodergren, S.; Solbrand, A.; Hagfeldt, A.; Lindquist, S.-E.; Wang, L. N.; Muhammed, M. *J. Phys. Chem. B* **1997**, *101*, 2598−2601.
(9) Dabestani, R.; Bard, A. J.; Campion, A.; Fox, M. A.; Mallouk, T. E.; Webber, S. E.; White, J. M. *J. Phys. Chem.* **1988**, *92*, 1872.
(10) Lencka, M. M.; Riman, R. E. *Ferroelectrics* **1994**, *151*, 159.
(11) Christensen, A. N.; Rasmussen, S. E. *Acta Chem. Scand.* **1963**, *17*, 845.
(12) Burnside, S. D.; Shklover, V.; Barbé, C.; Comte, P.; Arendse-Duriaux, F.; Brooks, K.; Grätzel, M. *Chem. Mater.* **1998**, *10*, 2419.
(13) Bolts, J. M.; Wrighton, M. S. *J. Phys. Chem.* **1976**, *80*, 2641.
(14) Kavan, L.; Grätzel, M.; Gilbert, S. E.; Klemenz, C.; Scheel, H. J. *J. Am. Chem. Soc.* **1996**, *118*, 6716−6723.
(15) Rothenberger, G.; Grätzel, M.; Fitzmaurice, D. *J. Phys. Chem.* **1992**, *96*, 5983.
(16) Enright, B.; Redmond, G.; Fitzmaurice, D. *J. Phys. Chem.* **1994**, *98*, 6195−6200.
(17) Moser, J. E.; Grätzel, M. *Chimia* **1998**, *52*, 160.
(18) Moser, J. E.; Wolf, M.; Lenzmann, F.; Grätzel, M. *Zeit. Phys. Chem.*, in print.
(19) Tachibana, Y.; Moser, J. E.; Grätzel, M.; Klug, D. R.; Durrant, J. R. *J. Phys. Chem.* **1996**, *100*, 20056.
(20) Humphry-Baker, R. unpublished data.
(21) Padilla, J.; Vanderbilt, D. *Surf. Sci.* **1998**, *418*, 64−70.
(22) Henrich, V. E.; Cox, P. A. *The Surface Science of Metal Oxides*; Cambridge University Press: Cambridge, 1994.
(23) Heifets, E.; Dorfman, S.; Fuks, D.; Kotomin, E.; Gordon, A. *J. Phys.: Condens. Matter* **1998**, *10*, L347-L353.
(24) Shklover, V.; Ovchinnikov, Yu. E.; Braginsky, L. S.; Zakeeruddin, S. M.; Grätzel, M. *Chem. Mater.* **1998**, *10*, 2533.
(25) Cohen, R.; Bastide, S.; Cahen, D.; Libman, J.; Shanzer, A.; Rosenwaks, Y. *Adv. Mater.* **1997**, *9*, 746−749.
(26) Kawasaki, M.; Takahasi, K.; Maeda, T.; Tsuchiya, R.; Shinohara, M.; Ishiyama, O.; Yonezawa, T.; Yoshimoto, M.; Koinuma, H. *Science* **1994**, *266*, 1540−1542.